Supplementary Information

Scalable Inverted Perovskite Solar Cells Enabled by Atomic Layer Deposition (ALD)

Aedan Gibson,[a,b] Canjie Wang,[a,b] Urasawadee Amornkitbamrung,[a,b] Yongjae In,[a,b] Seokhoon Han,[b,c] Hyeon Jun Jeong,[a,b] Hyun Suk Jung,[d,e] and Hyunjung Shin*[a,b,e]

[a]Department of Energy Science, [b]Nature Inspired Materials Processing Research Center, [c]Department of Future Energy Engineering, [d]School of Advanced Materials Science and Engineering, [e]SKKU Institute of Energy Science and Technology (SIEST), Sungkyunkwan University, Suwon 440-746, Republic of Korea

E-mail: hshin@skku.edu

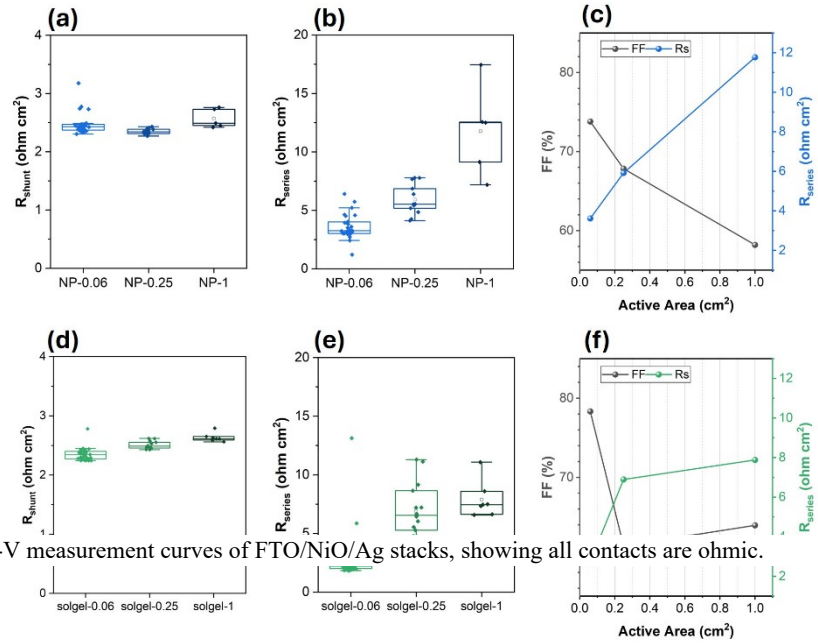

Figure S3. Linear I-V measurement curves of FTO/NiO/Ag stacks, showing all contacts are ohmic.

Figure S1. Dependence of resistive parameters and FF on device area in NP (blue, a-c) and sol-gel (green, d-f) NiO HTL-based iPSCs. Box plots showing the evolution of (a,d) shunt resistance (R_{sh}) and (b,e) series resistance (R_s) for device areas of 0.06, 0.25, and 1 cm^2. (c,f) Relationship between FF & R_S with increasing active area.

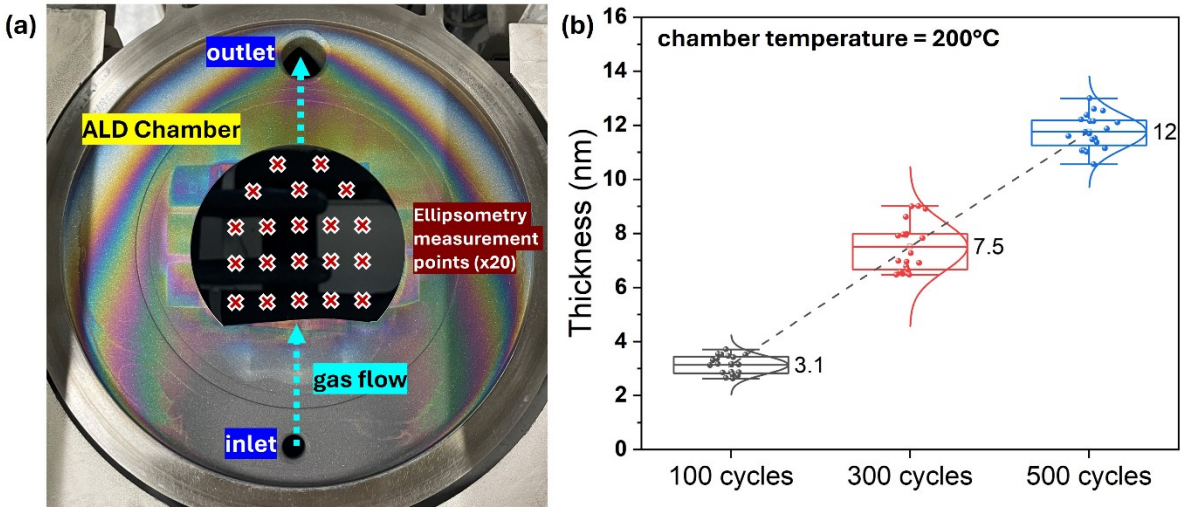

Figure S2. (a) Annotated photograph of the 4" silicon wafer loaded in the ALD chamber. (b) Thickness distribution of NiO films deposited at 200 °C for 100, 300, and 500 cycles. The dashed line represents the linear regression fit, yielding a growth-per-cycle (GPC) of 0.22 Å/cycle.

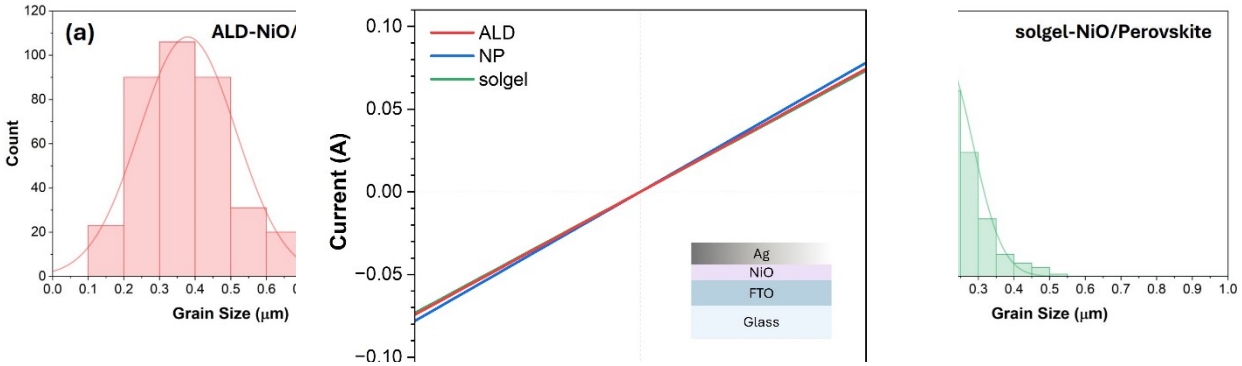

Figure S6. Perovskite grain size histograms on (a) ALD-NiO, (b) NP-NiO, and (c) solgel-NiO. ALD-NiO produces the largest grains, followed by NP-NiO and solgel-NiO. Grain sizes were quantified measuring five diameters per grain across entire SEM images using the program 'ImageJ'.

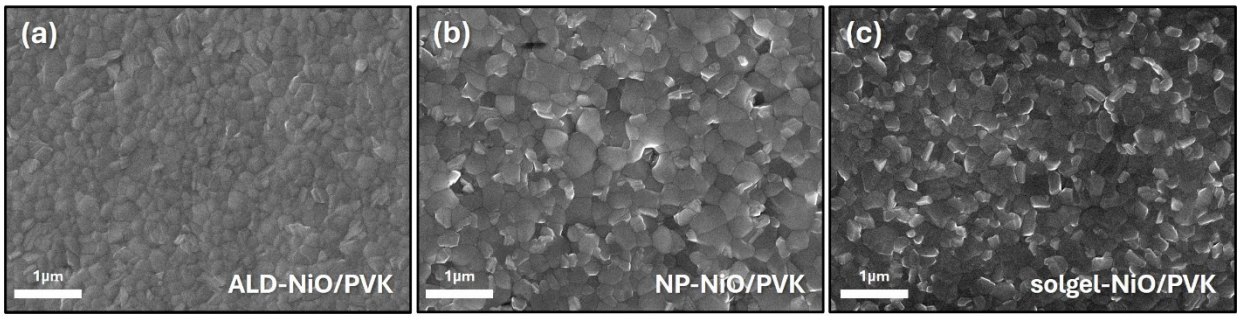

Figure S4. Topographical SEM images of perovskite deposited above (a) ALD-NiO, (b) NP-NiO, and (c) solgel-NiO HTLs.

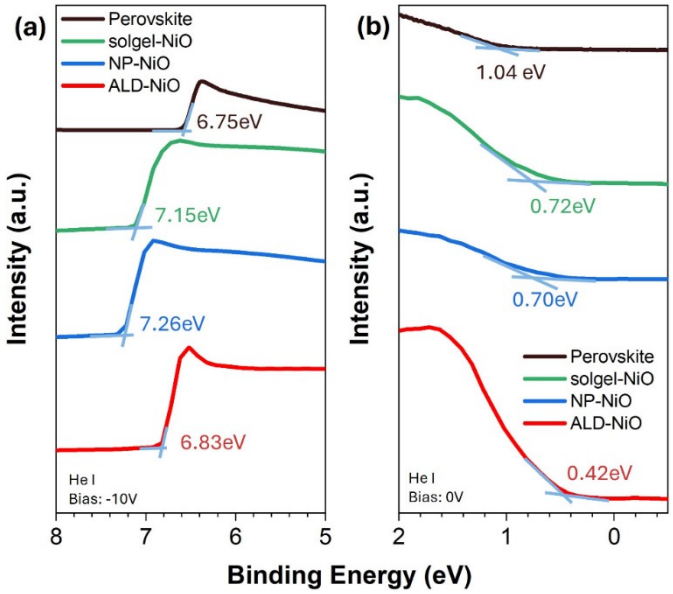

Figure S5. UPS spectra of (a) the secondary electron cutoff region, and (b) Fermi edge region for FTO/ALD-NiO (red), FTO/NP-NiO (blue), and FTO/solgel-NiO (green) with respect to perovskite (brown) as a reference.

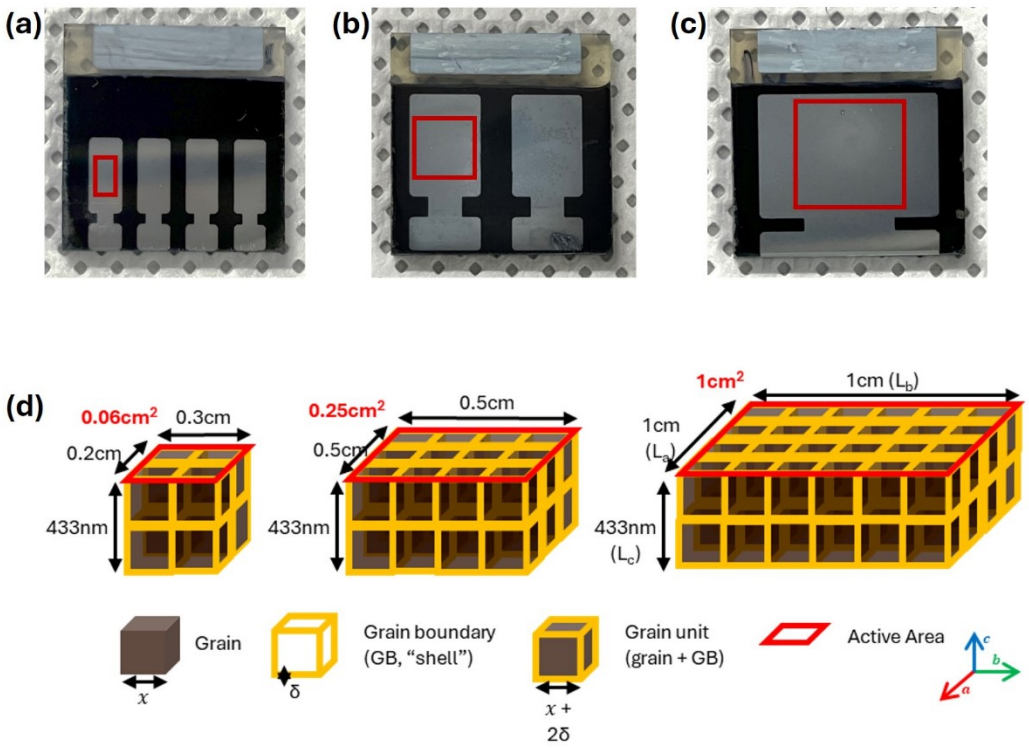

Figure S7. Top-view images of iPSC devices with active areas of (a) 0.06 cm^2 (b) 0.25 cm^2, and (c) 1 cm^2 (approximate active area shown by red boxes). (d) Schematic of 3D model of perovskite layer used to calculate total number of grains and total internal GB area within the perovskite layer.

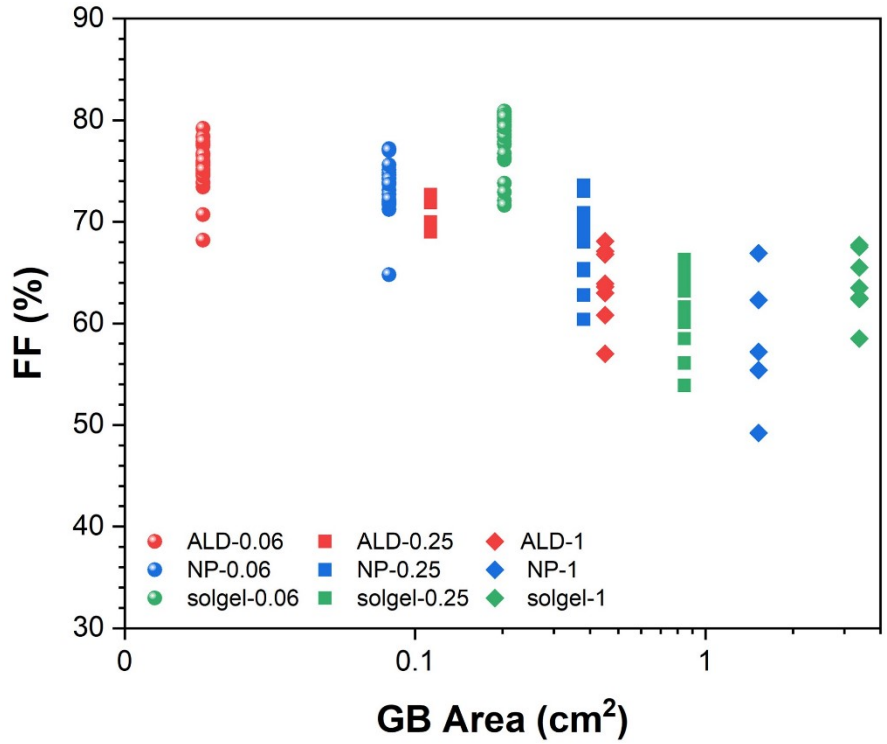

Figure S8. Fill Factor (measured) vs. Total Internal Grain Boundary Area (calculated from 3D perovskite model).

Active Area (cm^2)	NiO-HTL Deposition Method	V_{OC} (V)	J_{SC} ($mAcm^{-2}$)	FF (%)	PCE (%)
0.06	ALD	1.02± 0.01 (1.04)	23.7±0.96 (25.0)	75.7±2.10 (79.2)	18.3±1.0 (19.8)
	NP	1.00±0.20 (1.10)	22.7±1.04 (24.1)	73.8±2.56 (77.2)	17.7±1.0 (19.5)
	sol-gel	1.01±0.01 (1.03)	23.8±0.67 (24.9)	78.2±2.39 (80.9)	18.6±0.9 (19.8)
0.25	ALD	1.03±0.01 (1.03)	25.5±0.34 (26.2)	70.7±1.38 (72.7)	18.3±0.5 (19.1)
	NP	0.99±0.01 (1.00)	23.3±0.46 (24.2)	67.8±3.71 (73.6)	15.7±1.1 (17.2)
	sol-gel	1.00±0.01 (1.01)	21.8±0.56 (22.1)	61.3±3.42 (65.8)	13.5±0.8 (14.8)
1	ALD	1.03±0.01 (1.04)	24.7±0.59 (25.2)	63.8±3.43 (68.1)	16.2±1.1 (17.6)
	NP	0.99±0.01 (1.01)	21.5±1.20 (22.8)	58.2±6.04 (66.9)	12.5±2.0 (15.0)
	sol-gel	1.02±0.00 (1.02)	20.9±0.50 (21.5)	63.9±3.01 (67.7)	13.6±0.7 (14.8)

Table S1. Photovoltaic parameters (V_{OC}, J_{SC}, FF, and PCE) of perovskite solar cells using ALD, nanoparticle (NP), and sol–gel NiO HTLs, measured at active areas of 0.06, 0.25, and 1 cm^2. Values in brackets indicate the champion device (highest PCE) from each set.

NiO-HTL Deposition Method	Thickness (nm)
ALD (200 cycles)	6.4±0.16
NP	14.62±0.12
sol-gel	8.64±0.22

Parameter	Symbol
grain edge length	x
grain boundary shell thickness	δ
grain unit edge length	x + 2δ
total number of grain units	N
total volume of perovskite film	V_{film}
volume of grain unit	V_{GU}

Table S2. Average thickness and standard deviation of NiO thin films deposited on silicon wafers. Thickness measurements were taken by ellipsometry.

volume of grain boundary 'shell'	V_{GB}
total grain boundary volume in film	V_{GB_tot}
length of film in 'a' direction	L_a
length of film in 'b' direction	L_b
length of film in 'c' direction	L_c
number of grains along the 'a' direction	N_a
number of grains along the 'b' direction	N_b
number of grains along the 'c' direction	N_c
total internal grain boundary area (non-corrected)	A_{GB}
total internal grain boundary area (corrected)	A_{GB_corr}

Geometric estimation of grain boundary (GB) area

A simple geometric model was employed to estimate trends in the total internal grain boundary (GB) volume and area of the perovskite films as a function of average grain size. The model is intended to provide qualitative insight into how changes in microstructure may influence the density of internal grain boundaries and does not represent a transport or recombination model.

Table S3. 3D Perovskite Model Parameters.

Model description and assumptions

The perovskite layer is modelled as a perfectly cubic array of grains. Each cubic grain, with a side length x, is surrounded by a uniform grain boundary (GB) ‘shell’ of thickness δ, resulting in a ‘grain unit’ (grain + shell) of total side length x+2δ. All grain units are uniform, isotropic and perfectly packed with no voids. The perovskite film is modelled as a cuboid with dimensions, along axes a, b, and c, where and are the edge lengths defining the active area, and represents

the layer thickness (schematic shown in Figure S7) was determined by averaging over 50 measurements from cross-sectional SEM images using the program 'ImageJ'.[57]

Grain number and grain boundary volume

The total number of grain units within the perovskite layer N is calculated by dividing film volume by grain unit volume:

$$N = \frac{V_{film}}{V_{GU}} = \frac{L_a \cdot L_b \cdot L_c}{(x + 2\delta)^3} \quad (1)$$

The grain boundary volume V_{GB} is calculated as the difference between grain unit and grain volume:

$$V_{GB} = V_{GU} - V_G = (x + 2\delta)^3 - x^3 \quad (2)$$

Therefore, the total grain boundary volume in the film V_{GB_tot} can be calculated by the following formula:

$$V_{GB\_tot} = N \cdot V_{GB} \quad (3)$$

Estimation of internal grain boundary area

Total internal GB area is estimated from a corrected bulk area formula:

$$A_{GB\_corr} = 3Nx^2\left[1 - \frac{1}{3}\left(\frac{1}{N_a} + \frac{1}{N_b} + \frac{1}{N_c}\right)\right], \quad (4)$$

where $N_a = \frac{L_a}{x},\ N_b = \frac{L_b}{x},\ N_c = \frac{L_c}{x}$

The proof for the above equation is presented below. The non-corrected total internal grain boundary area can be given by the following formula:

$$A_{GB} = 3Nx^2 \quad (5)$$

In a real perovskite film, some grain units touch the surface, meaning that some faces are external. These external faces are considered part of the interfaces between layers, not grain boundaries. As such, they are considered to not contribute to the total internal GB area. Consider that along the direction, there are grains, and that the two end faces along the direction are external. As such, the fraction of internal faces along the direction can be given by:

(6)

$$\frac{total\ no.\ of\ internal\ faces\ along\ a}{total\ no.\ of\ grains\ along\ a} = \frac{N_a - 1}{N_a} = 1 - \frac{1}{N_a}$$

Similarly, in the b and c directions:

$$1 - \frac{1}{N_b} \quad (7) \qquad 1 - \frac{1}{N_c} \quad (8)$$

Since each grain contributes faces along all three axes, the model applies an average correction factor over the a, b and c directions to account for faces exposed at the film surface. The average total fraction of faces that are internal is given by:

$$\frac{\left(1 - \frac{1}{N_a}\right) + \left(1 - \frac{1}{N_b}\right) + \left(1 - \frac{1}{N_c}\right)}{3} = 1 - \frac{1}{3}\left(\frac{1}{N_a} + \frac{1}{N_b} + \frac{1}{N_c}\right) \quad (9)$$

Applying this correction to the total internal grain boundary area provides the proof for Equation (4).

$$A_{GB\_corr} = 3Nx^2\left[1 - \frac{1}{3}\left(\frac{1}{N_a} + \frac{1}{N_b} + \frac{1}{N_c}\right)\right],$$

where $N_a = \frac{L_a}{x},\ N_b = \frac{L_b}{x},\ N_c = \frac{L_c}{x}$

Results from calculations using this model are presented in Table S4 below.

Model limitations

This model assumes idealized cubic grain geometry, uniform grain size, and perfect packing, and does not account for grain size distributions, irregular grain shapes, voids, or preferential orientation. The calculated values should therefore be interpreted as relative trends rather than absolute descriptors of the microstructure.

HTL deposition method	Mean Grain Size, x (μm)	Active Area (cm^2)	Estimated No. of Grains (N)	Total Internal GB Area (cm^2)
ALD	0.38±0.14	0.06	4.36×10^7	0.027
		0.25	1.82×10^8	0.113
		1	7.27×10^8	0.451
NP	0.29±0.10	0.06	9.49×10^7	0.091
		0.25	3.96×10^8	0.380

		1	1.58×10^9	1.522
solgel	0.20±0.08	0.06	2.70×10^8	0.203
		0.25	1.13×10^9	0.845
		1	4.50×10^9	3.382

Table S4. Calculated values derived from the geometric perovskite grain model described above for films deposited on ALD, NP, and sol–gel NiO substrates. The model uses the experimentally determined mean grain sizes to estimate the total number of grains and the corresponding internal grain boundary (GB) area as a function of active area. Perovskite films grown on ALD NiO exhibit the largest mean grain size, followed by NP and sol–gel NiO, which results in a lower estimated internal GB area across all device areas. These values are intended to illustrate relative trends rather than absolute microstructural quantities.

NiO-HTL Deposition Method	Active Area (cm^2)	PCE (%)	Date	Reference
ALD (this work)	0.06	19.8	2026	n/a
	0.25	19.1		
	1	17.6		
e-Beam	0.105	15.4	2019	58

	2.3	12.4		
ECD	0.1	19.2	2017	59
	1.084	17		
Inkjet printing	0.105	17.2	2020	60
	1	12.3		
Magnetron Sputtering **HTL Configuration* (Sputtered-NiO/NP-NiO/SAM)	0.09	21.97	2023	61
	58.14	19.71		
	61.26	18.17		
	348.84	17.4		
Meniscus Coating (NP)	0.16	22.1	2021	62
	25	16.12		
Slot-die coating	0.14	17.33	2021	63
	2.1	14.9		

Note: ALD = Atomic Layer Deposition; e-Beam = Electron Beam Evaporation; ECD = Electrochemical deposition; NP = Nanoparticle.

Table S5. Summary of photovoltaic performance as a function of active area for inverted perovskite solar cells (iPSCs) employing various NiO-HTL deposition methods. This data corresponds to the scaling comparison presented in Figure 8d. The referenced works represent reports that utilise nominally identical architectures at different active areas to evaluate upscaling behaviour. Some reports employ multi-layer HTL/SAM configurations, as well as perovskite layer passivation.